JAST, Vol. 7, No. 2, pp 69–79
© Iranian Aerospace Society, Summer-Fall 2010

JAST
Journal of Aerospace Science and Technology

Numerical Predictions of Turbulent Mixed Convection Heat Transfer to Supercritical Fluids Using Various Low Reynolds Number k-ε Turbulence Models

M. Mohseni[1] and M. Bazargan[2]

There are a number of systems in which supercritical cryogenic fluids are used as coolants or propellant fluids. In some modern military aircraft, the fuel is pressurized above its critical point and used as a coolant to remove heat from the aircraft engine. Accurate prediction of heat transfer coefficients to turbulent flows of supercritical fluids is essential in design of such systems. One of the most challenging parts in mathematical modeling of this phenomenon is the turbulence modeling. The turbulence modeling, like other aspects of the supercritical fluid flows, seems to be highly affected by the large variations of the fluid properties. A two dimensional CFD code has been developed in this study and a number of the Low Reynolds Number (LRN) $k-\varepsilon$ turbulence models have been examined. Both flow conditions corresponding to the heat transfer enhancement and deterioration have been studied. The results appear to be quite sensitive to the choice of the turbulence model, especially in the deteriorated regime of heat transfer. The turbulence model assisting the two-dimensional numerical model of the present study to best fit the experiments has been determined for both cases of the enhanced and deteriorated heat transfer. That is while the jump in the wall temperature occurring in the deteriorated regime of heat transfer is over- predicted by the present numerical code regardless of the turbulence model used.

NOMENCLATURE

C_p	Specific heat capacity at constant pressure (J.kg^{-1}.K^{-1})
$C_{\varepsilon 1}, C_{\varepsilon 2}$	Constants in the ε equation
C_μ	Constant in μ_t relation
f_1, f_2	Functions in ϵ equation
f_μ	Damping function in μ_t relation
g	Gravitational acceleration (m.s^{-2})
G	Mass flux (kg.s^{-1}.m^{-2})
G_k	Turbulent production due to buoyancy (kg/m^{-1}.s^{-3})
h	Heat transfer coefficient (W.m^{-2}.K^{-1})
H	Enthalpy (J.kg^{-1})
k	Turbulent kinetic energy (m^2.s^{-2})
K_v	Non-dimensional acceleration parameter
P	Pressure (N.m^{-2})
P_k	Turbulent production due to shear stresses (kg/m^{-1}.s^{-3})
Pr	Molecular Prandtl number
Pr_t	Turbulent Prandtl number
q	Heat flux (W.m^{-2})
Q	Heat transfer rate (W)
r	Transversal direction of flow (m)

1. *Research Assistant, Ph.D., Dept. of Mech. Eng., K.N.Toosi University of Technology, Tehran, Iran, Email: m_mohseni@dena.kntu.ac.ir.*
2. *(Corresponding Author), Associate Professor, Dept. of Mech. Eng., K.N.Toosi University of Technology, Tehran, Iran, Email: bazargan@kntu.ac.ir.*

Re	Reynolds number
Re_t	Turbulent Reynolds number
S_k	Source term in k equation
S_ε	Source term in ε equation
T	Temperature (K)
u, v	Velocity components in x and r direction ($\mathrm{m.s^{-1}}$)
x	Axial direction of flow (m)
y^+	Non-dimensional distance from wall

Greek Symbols

β	Thermal expansion coefficient $(1/K)$
ϵ	Dissipation rate of $k(\mathrm{m^2/s^3})$
ψ	Dissipation function in energy equation $(1/\mathrm{s^2})$
ϕ	General field variable
λ	Thermal conductivity (W/m.K)
μ	Molecular viscosity (kg/m.s)
μ_t	Turbulent viscosity (kg/m.s)
ρ	Density $(\mathrm{kg/m^3})$
$\sigma_k, \sigma_\varepsilon$	Turbulent Prandtl numbers for k and ε equations (constant)
τ	Shear stress $(\mathrm{N/m^2})$

Subscript

b	Bulk
pc	Pseudo-critical
t	Turbulent
w	Wall

INTRODUCTION

At supercritical pressures, thermodynamic and transport properties of fluids change dramatically near the critical temperature. Figure 1 shows the typical variations of the properties of carbon dioxide at supercritical pressure of 8.12 MPa. For a given supercritical pressure, the temperature at which the fluid specific heat capacity is maximum is called the pseudo-critical temperature. Because of large property variations, heat transfer rates are dramatically enhanced near the critical region.

In most supercritical fluid flows, heat transfer is enhanced near the critical region. Under certain conditions, however, heat transfer may deteriorate. The buoyancy and flow acceleration effects are considered to be the main causes of the heat transfer degradation [1-7]. The buoyancy and flow acceleration are promoted due to large variations of the fluid density near the critical region. These two effects may cause the velocity profile to change. Consequently, the shear stress distribution and turbulence production vary and the re-laminarization of the flow may occur which leads to deterioration in heat transfer.

Despite extensive investigations carried out over the past few decades, there are large discrepancies between the results of various numerical studies attempting to predict the heat transfer coefficients in heat transfer to supercritical fluids (SCFs) [5-16]. The difficulty in turbulence modeling, especially in the near wall region, is considered to be one of the main sources of such discrepancies. The deteriorated regime of heat transfer which is usually due to the buoyancy effects, in particular, is more complicated and difficult to model. That is because the variations of the fluid properties at supercritical conditions are so large that the onset of the buoyancy effects occurs much earlier than expected in comparison to the flows at normal pressures.

In this study, a number of LRN $k-\epsilon$ turbulence models have been examined. To accomplish this, a two-dimensional CFD code is developed to simultaneously solve the governing equations in an upward flow of supercritical fluids in a round tube. Both improved and degraded modes of heat transfer are studied. Comparison of the results of the present study obtained via implementation of different turbulence models as well as their comparison with available experimental data is expected to help better understanding of the complicated phenomenon of heat transfer to supercritical fluid flows.

APPLICATION OF SUPERCRITICAL FLUIDS IN AERONAUTICAL SYSTEMS

The considerable enhancement of heat transfer at the supercritical conditions alongside the alteration of some characteristics of the fluid has resulted in an increase in the utilization of supercritical fluids in engineering systems within the past several decades. Some examples are the application of the supercritical fluids in fossil fuel and nuclear power plants, the

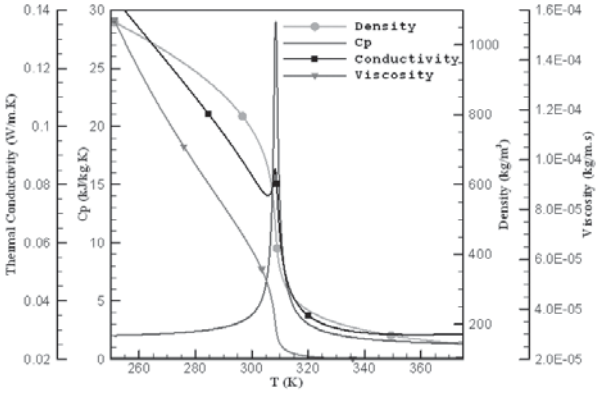

Figure 1. Typical variations of the properties of carbon dioxide at supercritical pressure of 8.12MPa.

chemical industry, and environmental engineering [1]. In aeronautical engineering, there are a number of applications in which supercritical cryogenic fluids are used as coolants or propellant fluids. Supercritical hydrogen, for example, is used as both the propellant and the heat sink in chemical and nuclear propulsion systems. In some modern military aircrafts, the fuel is pressurized above its critical point and used as a coolant to remove heat from the aircraft engine.

The advantages of the cooling effect of the supercritical fluids are more appreciated when we know that unlike other methods of enhancement of heat transfer, the pressure loss of the cooling fluid does not increase any further. It should be noted that the chamber and the nozzle must be cooled due to the high temperatures of the propellant combustion. As an example, one can note the temperature of a space shuttle's main engine, which, during firing, can reach as high as 3500 K. Thus, it is necessary to protect the surface of the nozzle and the combustion chamber from the eroding effects that high-pressure and high-temperature gases may create.

Before the propellants are injected into the combustion chambers, regenerative cooling systems cool the thrust chambers by conducting them as coolant through passages in the wall. This method is the most commonly used method. An expander cycle liquid rocket engine can be seen in Figure 2. At temperatures lower than the critical temperature (T_{cr}=33K), and with pressures above the critical point (P_{cr}=1.3 MPa), hydrogen enters the cooling channels where it is quickly heated to a supercritical gas as it passes through.

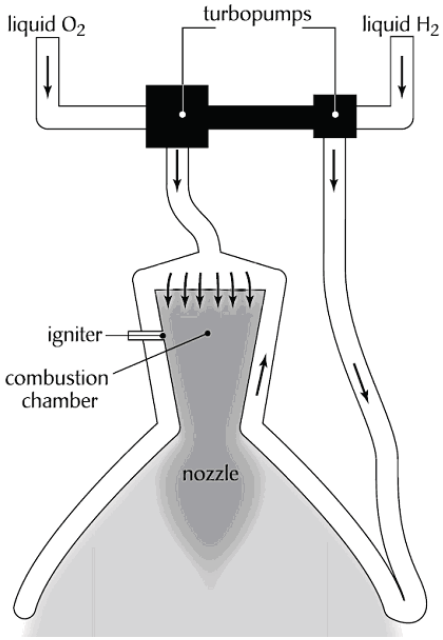

Figure 2. A simplified liquid-propellant rocket engine that employs regenerative cooling of the combustion chamber and nozzle walls [17].

In an expander cycle engine, one of the keys to achieving a successful engine configuration is heat transfer to the hydrogen coolant. The higher the rate of heat transfer to the coolant is, the higher the rate of enthalpy extraction in the turbo-machinery will be, and thus, the higher the operating pressures and/or thrust will become. Nonetheless, accurate design analysis predictions cannot be made due to the insufficient quantification of exact mechanisms through which enhanced heat transfer takes place. As the development of systems operating at supercritical pressures continues, this problem needs to be revisited more accurately. The optimal design of such systems requires a thorough understanding of the heat transfer encountered.

NUMERICAL MODELING

In the following, the governing equations applied to model the convective heat transfer to turbulent flow of a supercritical fluid in a vertical round tube have been described. The basic governing equations including the conservations of mass, momentum and energy, together with transport equations modeling the turbulence are employed to model the flow. Note that the flow is considered steady state and thus, the temporal terms have been eliminated. The conservation of mass states that:

$$\frac{\partial(\rho u_i)}{\partial x_i} = 0 \tag{1}$$

For turbulent flows, by using the Reynolds time averaging method, the momentum equation results in:

$$\frac{\partial}{\partial x_j}(\rho u_i u_j) = \rho g_i - \frac{\partial P}{\partial x_i} + \frac{\partial \tau_{ij}}{\partial x_j} + \frac{\partial}{\partial x_j}\left(-\rho\overline{u_i' u_j'}\right) \tag{2}$$

where

$$\tau_{ij} = \mu\left(\frac{\partial u_i}{\partial x_j} + \frac{\partial u_j}{\partial x_i} - \frac{2}{3}\delta_{ij}\frac{\partial u_k}{\partial x_k}\right) \tag{3}$$

By using the Boussinesq theorem, the turbulent shear stress can be found from the following equation in which the Reynolds stresses are related to the average velocity gradient.

$$-\rho\overline{u_i' u_j'} = \mu_t\left(\frac{\partial u_i}{\partial x_j} + \frac{\partial u_j}{\partial x_i} - \frac{2}{3}\delta_{ij}\frac{\partial u_k}{\partial x_k}\right) - \frac{2}{3}\delta_{ij}\rho k \tag{4}$$

where the symbols with primes denote the fluctuation components of the corresponding quantities. The energy equation in terms of enthalpy will be in the form of:

$$\frac{\partial}{\partial x_i}(\rho u_i H) = \frac{\partial}{\partial x_i}\left(\lambda\frac{\partial T}{\partial x_i} + \frac{\mu_t}{\mathrm{Pr}_t}\frac{\partial H}{\partial x_i}\right) + u_i\frac{\partial P}{\partial x_i} + \dot{Q} + \varphi \tag{5}$$

In the above equation, as in the momentum equation, the Boussinesq assumption has been used for modeling turbulent heat flux.

The dissipation function can be written as follows:

$$\varphi = \left(\frac{\partial u_i}{\partial x_j} + \frac{\partial u_j}{\partial x_i} - \frac{2}{3}\delta_{ij}\frac{\partial u_k}{\partial x_k}\right)\frac{\partial u_i}{\partial x_j} \tag{6}$$

For calculating the convective heat transfer coefficient, Newton[s cooling law is used as below:

$$h = \frac{q_w}{T_w - T_b} = \frac{\lambda}{T_w - T_b}\frac{\partial T}{\partial r}\bigg|_w \tag{7}$$

The two-dimensional model developed in this study is used to examine six different LRN $k-\varepsilon$ turbulence models suggested by various researchers. The turbulence models implemented are those of Jones and Launder (JL) [18], Launder and Sharma (LS) [19], Chien (CH) [20], Myong and Kassagi (MK) [21], Abe, Kondoh and Nagano (AKN) [22], and Cotton and Kirwin (CK) [23]. The general form of the aforementioned models is as follows:

$$\frac{\partial}{\partial x_i}(\rho u_i k) = \frac{\partial}{\partial x_i}\left[\left(\mu + \frac{\mu_t}{\sigma_k}\right)\frac{\partial k}{\partial x_i}\right] + P_k + G_k - \rho\varepsilon - \rho S_k \tag{8}$$

$$\frac{\partial}{\partial x_i}(\rho u_i \varepsilon) = \frac{\partial}{\partial x_i}\left[\left(\mu + \frac{\mu_t}{\sigma_\varepsilon}\right)\frac{\partial \varepsilon}{\partial x_i}\right] + C_{\varepsilon 1} f_1 \frac{\varepsilon}{k}(P_k + G_k) - C_{\varepsilon 2} f_2 \rho \frac{\varepsilon^2}{k} + \rho S_\varepsilon \tag{9}$$

The following relationship is used to calculate the eddy viscosity:

$$\mu_t = \rho C_\mu f_\mu \frac{k^2}{\varepsilon} \tag{10}$$

We also have:

$$P_k = -\rho\overline{u_i' u_j'}\frac{\partial u_i}{\partial x_j} \tag{11}$$

and

$$G_k = 0.3\beta g_i \frac{k}{\varepsilon}\left(-\rho\overline{u_i' u_j'}\frac{\partial T}{\partial x_j}\right) \tag{12}$$

The Eq. (12) is obtained from the GGDH (Generalized Gradient Diffusion Hypothesis) modeling assumption. The details on GGDH may be found in literature [24]. The specifications of the turbulence models including functions, coefficients and boundary conditions in turbulence models are listed in Tables 1 to 3.

In contrast with the high Reynolds number turbulence models, there is no need for the wall functions to bridge between the core and the near wall regions in the LRN $k-\varepsilon$ models. The LRN models use damping functions instead to account for the near wall effects. The damping functions, if implemented properly, bring about the opportunity of modeling a broader range of the flow fields. The limitations imposed by the wall functions are described in [25].

The large variations of the fluid properties in supercritical conditions lead the equations of momentum and energy to become highly coupled. Thus, the convergence of the solutions to the equations is more difficult to reach. The proper choice of underrelaxation factors (URFs) is essential. Generally speaking, the smaller values of URFs are needed comparing to the constant property flows. Too large values of URFs may lead to oscillatory or even divergent iterative solutions especially at high heat fluxes and a value which is too small will cause extremely slow convergence. This phenomenon also necessitates the greater number of meshes to be used, especially in radial direction, compared to the cases at normal pressures (constant property flows). Thus, more calculating power is required to deal with such highly variable property flows.

More explanations about the structure of the present code can be found in a previous study by Bazargan and Mohseni [26].

RESULTS

In order to evaluate the results of the present study, the experimental data, the geometry and boundary conditions applied by Song *et.al.* [27] for carbon dioxide and Bazargan *et.al.* [2] for water have been chosen. A summary of the flow conditions is stated in Table 4. Note that the pseudo critical temperature and pressure of carbon dioxide are T=304.13 K and P=7.37 MPa respectively. The pseudo critical temperature and pressure of water are also T=647.1 K and P=22.06 MPa

Table 1. Functions, coefficients and boundary conditions in JL and LS $k-\epsilon$ models.

Quantity	JL model	LS model
f_1	1	1
f_2	$[1-0.3\exp(-Re_t^2)]$	$[1-0.3\exp(-Re_t^2)]$
f_μ	$\exp\left(-\frac{2.5}{1+Re_t/50}\right)$	$\exp\left(-\frac{3.4}{(1+Re_t/50)^2}\right)$
S_k	$2\ \nu\left(\partial\sqrt{(k)}/\partial y\right)^2$	$2\ \nu\left(\partial\sqrt{(k)}/\partial y\right)^2$
S_ϵ	$2\ \nu\nu_t\left(\partial^2 u/\partial y^2\right)^2$	$2\ \nu\nu_t\left(\partial^2 u/\partial y^2\right)^2$
k_w	0	0
ε_w	0	0
C_μ	0.09	0.09
$C_{\varepsilon 1}$	1.45	1.44
$C_{\varepsilon 2}$	2	1.92
σ_k	1	1
σ_ε	1.3	1.3

respectively. For the calculation of the thermodynamic properties of supercritical fluid, the NIST database [28] has been used. It should be noted that the experimental heat transfer data available in the literature for supercritical carbon dioxide and supercritical water are larger than those of supercritical hydrogen. Thus, supercritical CO2 and supercritical H2O have been used in this study to facilitate the comparison of the model predictions against experiments. The results of the model developed in this study are equally valid for supercritical CO2, supercritical H2 and other SCFs.

The effects that turbulence modeling can have on both the enhanced and degraded regimes of heat transfer are discussed below.

Enhanced Regime of Heat Transfer

Figure 3 shows the heat transfer coefficients obtained by making use of different turbulence models for CASE 1. The experimental data of Song *et.al.* [27] are also shown for the sake of comparison. As can be seen, the general trend of variations of the heat transfer coefficients predicted by various models is similar. The peak values of the heat transfer coefficients, however, differ noticeably. Comparison with the experiments show that making use of the CK, MK and CH turbulence models lead to more accurate results. That is while implementation of the JL and the LS turbulence models leads to the largest (18.3 kW/m2.K) and the lowest (10.5 kW/m2.K) peak values for the heat transfer coefficients respectively.

Note that it is a common practice, in presenting the heat transfer data of supercritical fluids, to use the fluid bulk enthalpy instead of bulk temperature for horizontal axis. For the constant heat flux condition, the equal differences of the values of bulk enthalpies correspond to equal distances along the tube. That is not the case for bulk temperature differences.

The numerical results for the heat transfer coefficients in the supercritical water for flow conditions of CASE 2 are shown in Figure 4. The similar type of dependency of the results on the turbulence models to that shown in Figure 3 for supercritical CO2 is repeated in Figure 4 for supercritical water. It should be noted that the test conditions of CASE 2 is for a horizontal flow. However, the buoyancy effect in test conditions of CASE 2 are negligible [2]. Thus, the flow is axisymetric

Table 2. Functions, coefficients and boundary conditions in MK and CH $k-\varepsilon$ models.

Quantity	MK model	CH model
f_1	1	1
f_2	$[1-0.22\exp(-Re_t^2/36)][1-\exp(-y^+/5)]^2$	$[1-0.22\exp(-Re_t^2/36)]$
f_μ	$[1-\exp\left(-y^+/70\right)]\left(1+3.45/Re_t^{0.5}\right)$	$1-\exp\left(-0.0115y^+\right)$
S_k	0	$2\ \nu\frac{k}{y^2}$
S_ε	0	$2\ \nu\frac{\varepsilon}{y^2}\exp\left(-0.5y^+\right)$
k_w	0	0
ε_w	$\nu\frac{\partial^2 k}{\partial y^2}$	0
C_μ	0.09	0.09
$C_{\varepsilon 1}$	1.4	1.35
$C_{\varepsilon 2}$	1.8	1.8
σ_k	1.4	1
σ_ε	1.3	1.3

Table 3. Functions, coefficients and boundary conditions in CK and AKN $k-\varepsilon$ models.

Quantity	CK model	AKN model
f_1	1	1
f_2	1	$\{1-0.3\exp[(-Re_t/6.5)^2]\}\left[1-\exp\left(-\frac{y^*}{3.1}\right)\right]^2$
f_μ	$1-0.97\exp\left(-\frac{\mathrm{Re}_t}{200}\right)-0.0045\mathrm{Re}_t\exp\left[-\left(\frac{\mathrm{Re}_t}{200}\right)^3\right]$	$\left\{1+\frac{5}{\mathrm{Re}_t^{0.75}}\exp\left[-\left(\frac{\mathrm{Re}_t}{200}\right)^2\right]\right\}\left[1-\exp\left(-\frac{y^*}{14}\right)\right]^2$
S_k	$2\ \nu\left(\frac{\partial\sqrt{k}}{\partial y}\right)^2$	0
S_ε	$0.95\nu\nu_t\left(\frac{\partial^2 u}{\partial y^2}\right)^2$	0
k_w	0	0
ε_w	0	$\nu\frac{k}{y^2}$
C_μ	0.09	0.09
$C_{\varepsilon 1}$	1.44	1.5
$C_{\varepsilon 2}$	1.92	1.9
σ_k	1	1
σ_ε	1.3	1.4

Table 4. Flow conditions examined in the present numerical model.

State	Fluid	p(MPa)	G(kg/m^2.s)	q(kW/m^2)	L(m)	D(mm)	Mode of heat transfer
CASE 1	CO2	8.12	1200	50	14	9	enhancement
CASE 2	H2O	25.2	965	307	7	6.3	enhancement
CASE 3	CO2	8.12	400	30	7	9	deterioration
CASE 4	CO2	8.12	400	50	5	9	deterioration

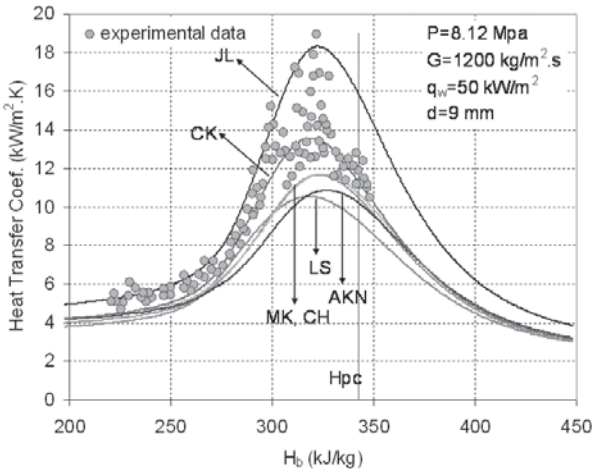

Figure 3. Comparison of the heat transfer coefficients predicted by the numerical code with the experiments of Song *et.al.* [27] for CASE 1.

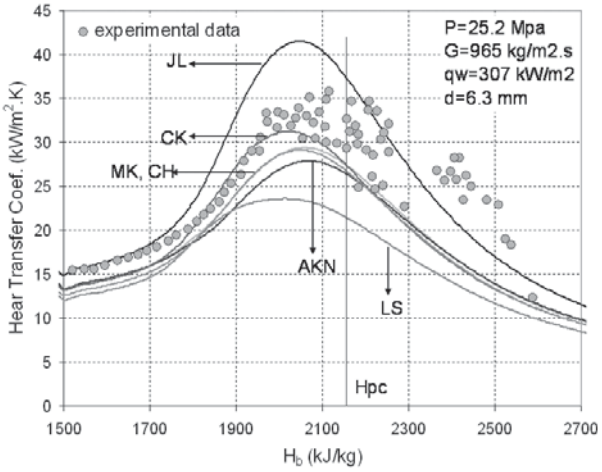

Figure 4. Comparison of the heat transfer coefficients predicted by the numerical code with the experiments of Bazargan *et.al.* [2] for CASE 2.

and the present numerical code is applicable to those conditions.

As shown in Figure 3 and Figure 4, the peak values of the heat transfer coefficients occur before the fluid bulk temperature reaches the pseudo-critical point. That is, as shown by Bazargan and Mohseni [26], due to the significance of the buffer zone of the boundary layer on convective heat transfer to the supercritical fluid flows. The explanation is that the numerical results indicate that in the enhanced regime of heat transfer, the peak of the heat transfer coefficients occurs when the pseudo-critical temperature, or the situation of maximum heat capacity, lies within the buffer layer.

As can be seen, the general form of the turbulence models used in the numerical simulation is similar. The main differences are due to the empirical constants and the damping functions. Such differences seem to be mainly responsible for the discrepancies among the results of the numerical simulations. The radial variations of the damping functions used in the various turbulence models for an arbitrary cross section of the flow are demonstrated in Figure 5. As shown, the damping functions have values near zero adjacent to the wall and approach the values near unity in the core region. In fact, the values near zero at the region close to the wall are the cause of the laminarization of the flow in the near wall region. That is because the wall functions have been eliminated in the LRN $k-\varepsilon$ turbulence models. The distance from the wall it takes the damping function to reach close to one affects the performance of the models noticeably. Not only the mentioned distance, but the way of variation of the damping functions from the wall to the log-law region matters.

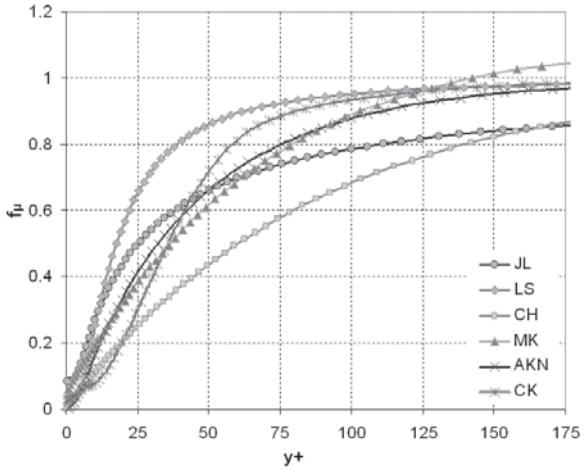

Figure 5. Variations of damping functions of different turbulence models in an arbitrary cross section of the flow predicted by the numerical code for CASE 2.

Deteriorated Regime of Heat Transfer

The results of the present model with various turbulence models for CASE 3 and CASE 4 are shown in Figure 6 and Figure 7 respectively. The experimental data of Song *et.al.* [27] are also shown for the sake of comparison. Both CASE 3 and CASE 4 represent the deteriorated regimes of heat transfer. It can be seen from Figure 6 and Figure 7 that the numerical results are in qualitative agreement with the experiments. That is, the numerical solutions clearly distinguish between the improved and degraded regimes of heat transfer. Quantitatively, however, there are large discrepancies between the numerical model and the experiments.

As shown in Figure 6 and Figure 7, the use of the MK turbulence model leads to the deteriorated heat transfer coefficients which are in better agreement with

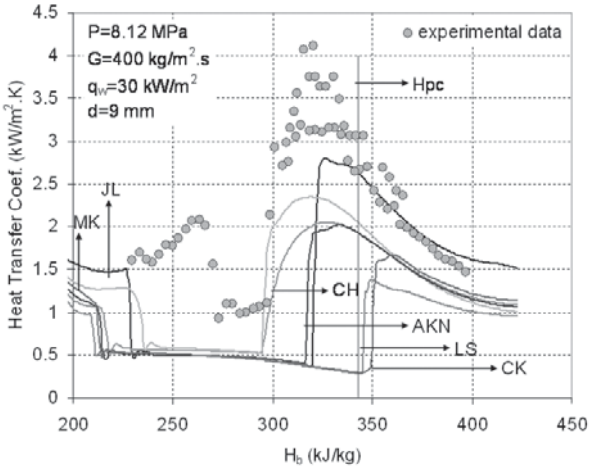

Figure 6. Comparison of the heat transfer coefficients predicted by the numerical code with the experiments of Song *et.al.* [27] for CASE 3.

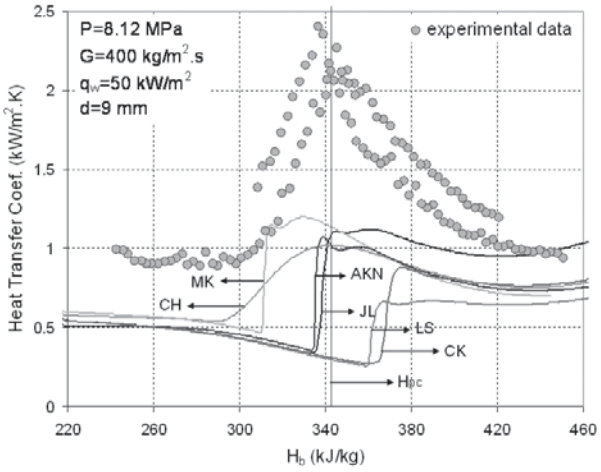

Figure 7. Comparison of the heat transfer coefficients predicted by the numerical code with the experiments of Song *et.al.* [27] for CASE 4.

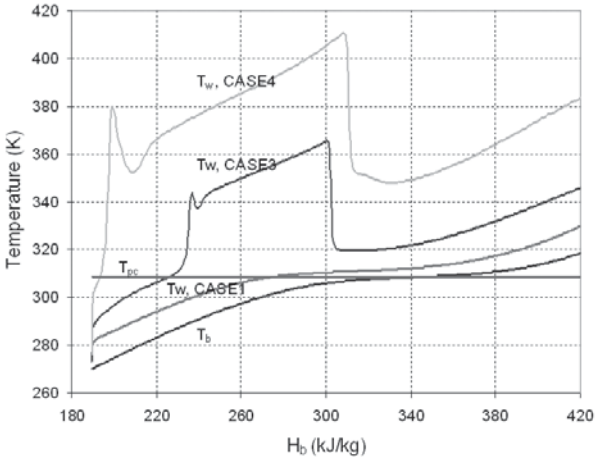

Figure 8. Variations of the wall temperature predicted by making use of the MK model for CASE 1, CASE 3 and CASE 4.

the experimental data, especially that it can predict the end of the deteriorated region of heat transfer more accurately. The results obtained by implementation of the turbulence models of CK and LS deviate the most from the experiments compared to the results of the numerical model with making use of the other turbulence models. The common fact observed in all the numerical results is that the zone of deteriorated heat transfer is predicted to be longer than what the experimental results suggest.

It should be noted that the heat flux in CASE 4 is greater than that of CASE 3. Thus, the deterioration in heat transfer occurs earlier in CASE 4. The peak of heat transfer coefficient is smaller in CASE 4 than in CASE 3. The variations of the predicted wall temperature by making use of the MK turbulence model for the CASE 1, CASE 3 and CASE 4 are shown in Figure 8. As shown in Figure 8, once the wall temperature approaches the pseudo-critical temperature in CASE 3 and CASE 4, a rapid increase in the wall temperature occurs which is a clear indication of deterioration in heat transfer. This behavior is observed regardless of the turbulence model used. The differences in the results are due to the extent of such rapid increases in the wall temperature. The available data in literature show that the deteriorated wall temperatures are usually being over-predicted.

It can be concluded from Figure 6 and Figure 7 that the available LRN $k-\varepsilon$ turbulence models are inadequate to accurately determine the turbulent activities and hence the rate of heat transfer in the deteriorated mode of convection to supercritical fluids. That is because the turbulence models generally depend highly on empirical parameters which have been developed for constant property flows. It is extremely difficult to measure turbulence in a flow at supercritical conditions. Extension of the application

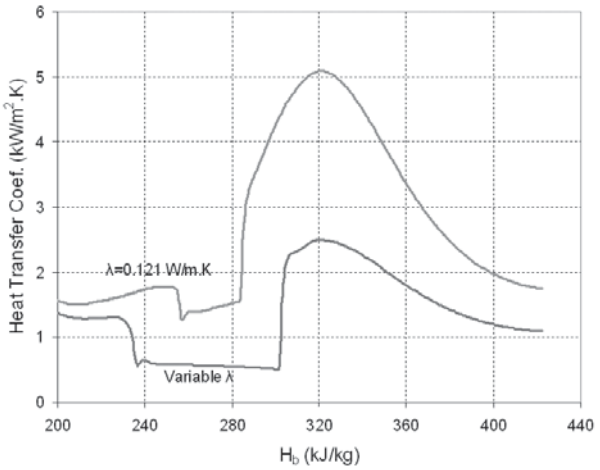

Figure 9. Variations of heat transfer coefficients for constant and variable fluid thermal conductivity by making use of the MK model for CASE 3.

of existing turbulence models to the case of highly variable property flow of the supercritical fluids is, at least for the deteriorated regime of heat transfer, under question.

In addition to the difficulty with turbulence modeling, there are also other factors which may account for the inaccurate prediction of the deteriorated heat transfer to the supercritical fluid flows. One example is the uncertainty existing with the choice of the turbulent Prandtl number, Pr_t. The results of Bazargan and Mohseni [29] show that, in the deteriorated regime of heat transfer, the implementation of the commonly used value of 0.9 for the Pr_t can effectively contribute to the existing errors in the predicted results.

It is worthwhile here to briefly comment on the effect of variations of the fluid thermal conductivity on heat transfer deterioration. It can be learnt from Figure 1 that the value of the thermal conductivity of the fluid decreases at the wall with an increase in T_w along the flow. For a constant value of the wall heat flux, from the Fourier's equation of heat conduction, $q_w = \lambda \partial T/\partial r|_w$, it is clear that the temperature gradient adjacent to the wall, and hence T_w, increases as the thermal conductivity decreases. However, once the ratio of the heat flux to the mass flow rate is low or moderate, the turbulence near the wall in the buffer layer is so aggravated due to large variations of the fluid properties that it overrules the effect of the decrease in thermal conductivity and the heat transfer improves. It means that no jump in the wall temperature will occur. At high heat fluxes, the reduction of the turbulent activities due to the buoyancy or the thermal acceleration effects and the decrease of the thermal conductivity assist each other and lead to deterioration of the heat transfer or equivalently the occurrence of the large values of the wall temperature. It is reasonable to state that the jump of the wall temperature in the course of the flow is partially due to the decrease of the thermal conductivity of the fluid.

This is further investigated numerically for the flow conditions of CASE 3 by assuming that the fluid thermal conductivity does not change and holds virtually its inlet value of $\lambda = 0.121$ W/m.K all along the course of the flow. That is while the other fluid properties vary with temperature as they naturally do so. The results so obtained for the heat transfer coefficients are compared with the normal case in which the conductivity is also a varying property and shown in Figure 9. As it is clear, the deterioration region is reduced and the values of heat transfer coefficients enhance considerably in comparison to the original case.

It is known that in the tubes with large or moderate diameters, similar to those used in this study, the effect of the thermal acceleration is negligible compared to the buoyancy effect. This can be appreciated from the work of McEligot *et.al.* [30] who studied the influence of the thermal acceleration and presented the parameter K_v, defined below, to consider this effect.

$$K_v = \frac{4\mu q_w}{C_p T_b dG^2} = \frac{4q_w^+}{\mathrm{Re}^2} \tag{13}$$

where

$$q_w^+ = \frac{q_w}{GC_b T_b} \tag{14}$$

They stated that when $K_v \leq 3 \times 10^{-6}$, the fluid flow remains turbulent while for higher values of K_v, *i.e.* for $K_v > 3 \times 10^{-6}$, the turbulence reduces and the flow relaminarization may occur. Lee *et.al.* [31] updated the above threshold value from 3×10^{-6} to 2.5×10^{-6}. K_v should be evaluated according to flow inlet conditions.

For the flow conditions used in this study, K_v has a maximum value of about 10^{-8}. Thus, according to the above criteria, the effect of the thermal acceleration on the rate of heat transfer is negligible and deterioration is mainly due to the buoyancy force.

It is useful to note that, in the governing equations, the buoyancy force affects the numerical results through two different ways. One is that the term G_k in the equations of k and ε (Eq. 12), *i.e.* the turbulent production due to buoyancy, appears as a result of interaction between the velocity and density fluctuations. The other factor shows itself via the source term, ρg, in the momentum equation. The source term leads to the increase of the fluid velocity near the wall (advection) in an upward flow. It results in flattening of the velocity profile. This causes the turbulence intensity of the flow to reduce. The opposite effect is expected to occur in a downward flow. The predicted results of the present study, not shown here,

indicate that the turbulent production due to the buoyancy (Eq. 12) is negligible with respect to the turbulent production due to shear stresses (Eq. 11). Thus, the effect that buoyancy has on the velocity profile may have the major contribution to the heat transfer impairment.

When the large increase in the wall temperature occurs which means the deterioration in heat transfer, the fluid density in the near wall region decreases further. This will cause the turbulent viscosity to decrease significantly and the flow becomes laminar locally. After the fluid is further heated in the course of the flow, the fluid density reduces which is as a result of temperature increase. However, the density in the near wall region decreases with a slower gradient with respect to the corresponding reduction in the core region. That is because the variations of the density with temperature are lesser at a higher temperature. In other words, the difference between the fluid density at the wall and in the core region reduces as shown in Figure 10. Meanwhile, the flow turbulence increases due to the turbulent production mechanisms. Furthermore, the bulk heat capacity approaches its pseudo-critical value. The increase of C_{pb}, in turn, will cause the temperature difference between the wall and bulk to reduce. All of the above together cause the wall temperature to decrease and the normal mode of heat transfer starts again.

CONCLUSIONS

In this study, the convective heat transfer to turbulent flow of a supercritical fluid is investigated numerically. A two-dimensional CFD code is developed to simultaneously solve the momentum and energy equations. In order to investigate the effect of turbulence models, six different Low Reynolds Number $k-\varepsilon$ models have been examined. The carbon dioxide and water at supercritical conditions are used to represent a fluid with highly variable properties. Both enhanced and deteriorated regimes of heat transfer are considered. The most important results of this study are as follow:

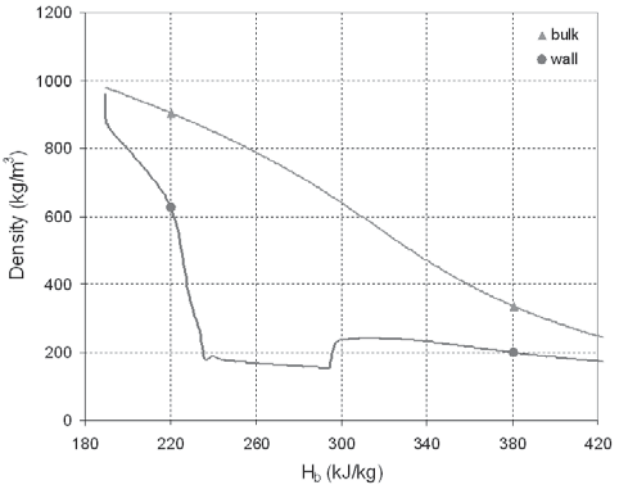

Figure 10. Variations of fluid density in the course of the flow by making use of the MK model for CASE 3.

1) The existence of the heat transfer enhancement can be predicted by the present numerical code regardless of the type of turbulence model used. The peak values of the heat transfer coefficients, however, differ noticeably. The comparison of the results with the experiments show that applying the CK, MK and CH turbulence models leads the present model to predict the heat transfer coefficients the best. The turbulence models of JL and LS lead to the maximum and minimum values of heat transfer coefficients, respectively.

2) Implementation of the various LRN $k-\varepsilon$ turbulence models in the present numerical model leads to qualitatively acceptable predictions of deterioration of heat transfer. Quantitatively, however, there exist noticeable disagreements among the results. They all over-predict both the length of the deterioration region as well as the wall temperatures. That is because the suppression of the turbulent activities near the wall is over-estimated. The turbulence model of MK results in best agreement with the experimental data. The end of the deteriorated region of heat transfer, in particular, has been more accurately predicted.

3) The main reason for discrepancies between the numerical results for heat transfer coefficients may be due to the difference in damping functions of LRN $k-\varepsilon$ turbulence models which causes the turbulent eddy viscosity to differ in various models.

4) The predicted results show that the increase of the wall temperature in the course of the heated flow is partially due to the decrease of the fluid thermal conductivity. In pipes with moderate or large diameters, as of the case considered in this study, the effect of thermal conductivity is even greater than the effect of the thermal acceleration in impairment of the heat transfer.

5) The effect of buoyancy in turbulence production (G_k in Eq. 12) is small compared to the turbulence production due to interactions of the Reynolds stresses and the mean velocity gradient (P_k in Eq. 11) even in the deteriorated regime of heat transfer. In an upward flow, the major effect of buoyancy which may contribute to the impairment of heat transfer is due to the flattening of the velocity profile, *i.e.* the decrease of velocity gradient through the source term in the x momentum equation.

REFERENCES

1. Bazargan M., and Fraser D., "Heat Transfer to Supercritical Water in A Horizontal Pipe: Modeling, New Empirical Correlation, and Comparison Against Experimental Data", *Journal of Heat Transfer*, **131**, (2009).

2. Bazargan M., Fraser D., and Chatoorgan V., "Effect of Buoyancy on Heat Transfer in Supercritical Water Flow in A Horizontal Round Tube", *Journal of Heat Transfer*, **127**, PP 897-902(2005).
3. Hall W.B., and Jackson J.D., "Laminarization of a Turbulent Pipe Flow by Buoyancy Force", *ASME Paper No. 69-HT-55* , (1969).
4. Jackson J.D., and Hall W.B., "Influences of Buoyancy on Heat Transfer to Fluids Flowing in Vertical Tubes under Turbulent Conditions", *Turbulent Forced Convection in Channels and Bundles*, PP 613-640 (1979).
5. Renz U., and Bellinghausen R., "Heat Transfer in A Vertical Pipe at Supercritical Pressure", *8th International Heat Transfer Conference*, **3**, PP 957-962 (1986).
6. Sharabi M., Ambrosini W., He S., and Jackson J.D., "Prediction of Turbulent Convective Heat Transfer to a Fluid At Supercritical Pressure In Square And Triangular Channels", *Annals of Nuclear Energy*, **35**(6), PP 993-1005 (2008).
7. He S., Kim W.S., and Bae J.H., "Assessment of Performance of Turbulence Models in Predicting Supercritical Pressure Heat Transfer in a Vertical Tube", *International Journal of Heat Mass Transfer*, **51**, PP 4659-4675(2008).
8. Malhortra A., and Hauptmann E.G., "Heat Transfer to Supercritical Fluid During Turbulent Vertical Flow in a Circular Duct", *International seminar on turbulent buoyant convection (ICGMT)*, Yugoslavia, (1976).
9. Cheng X., Kuang B., and Yang Y.H., "Numerical Analysis of Heat Transfer in Supercritical Water Cooled Flow Channels", *Nuclear Engineering and Design*, **237**, PP 240-252(2007).
10. Lee S.H., "Transient Convective Heat Transfer to Water Near The Critical Region in a Vertical Tube", *International Communications in Heat and Mass Transfer*, **33**, PP 610-617(2006).
11. Masuda Y., Suzuki A., and Ikushima Y., "Calculation Method of Heat and Fluid Flow in a Microreactor for Supercritical Water and Its Solution", *International Communications in Heat and Mass Transfer*, **33**, PP 419-425(2006).
12. Yang J., Oka Y., Ishiwatari Y., Liu J., and Jaewoon Y., "Numerical Investigation of Heat Transfer in Upward Flows of Supercritical Water in Circular Tubes and Tight Fuel Rod Bundles", *Nuclear Engineering and Design*, **237**, PP 420-430(2007).
13. Kim S.H., Kim Y.I., Bae Y.Y., and Cho B.H., "Numerical Simulation of the Vertical Upward Flow of Water in a Heated Tube at Supercritical Pressure", *Proceeding of International Congress on Advances in Nuclear Power Plants (ICAPP)*, (2004).
14. He S., Kim W.S., and Jackson J.D., "A Computational Study of Convective Heat Transfer to Carbon Dioxide at a Pressure Just Above the Critical Value", *Applied Thermal Engineering*, **28**(13), PP 1662-1675(2008).
15. Jiang P.X., Zhang Y., and Shi R.F., "Experimental and Numerical Investigation of Convection Heat Transfer of CO2 at Supercritical Pressures in a Vertical Mini-Tube", *International Journal of Heat Mass Transfer*, **51**, PP 3052-3056(2008).
16. Jiang P.X., Zhang Y., Zhao C.R., and Shi R.F., "Convection Heat Transfer of CO2 at Supercritical Pressures in a Vertical Mini Tube at Relatively Low Reynolds Numbers", *Experimental Thermal and Fluid Sciences*, **32**, PP 1628-1637(2008).
17. Angelo J.A., *Rockets*, Facts on Files Inc., (2006).
18. Jones W.P., and Launder B.E., "The Prediction of Laminarization with a Two-Equation Model of Turbulence", *International Journal of Heat and Mass Transfer*, **15**, PP 301-314(1972).
19. Launder B.E., and Sharma B.L., "Application of The Energy-Dissipation of Turbulence to Calculation of Flow Near a Spinning Disc", *Letters in Heat and Mass Transfer*, **1**, PP 131-138(1974).
20. Chien K.Y., "Predictions of Channel and Boundary-Layer Flows with a Low-Reynolds Number Turbulence Model", *AIAA Journal*, **20**, PP 33-38(1982).
21. Myong H.K., and Kasagi N., "A New Approach to the Improvement Of $k-\epsilon$ Turbulence Model for Wall Bounded Shear Flows", *JSME International Journal*, **33**, PP 63-72(1990).
22. Abe K., Kondoh T., and Nagano Y., "A New Turbulence Model for Predicting Fluid Flow and Heat Transfer in Separating and Reattaching Flows-L. Flow Field Calculations", *International Journal of Hear mass Transfer*, **37**, PP 139-151(1994).
23. Cotton M.A., and Kirwin P.J., "A Variant of the Low-Reynolds-Number Two-Equation Turbulence Model Applied to Variable Property Mixed Convection Flows", *International Journal of Heat and Fluid Flow*, **16**, PP 486-492(1995).
24. Kim W.S., He S., and Jackson J.D., "Assessment by Comparison With DNS Data of Turbulence Models Used in Simulations of Mixed Convection", *International Journal of Heat and Mass Transfer*, **51**, PP 1293-1312(2008).
25. Wilcox D.C., *Turbulence modeling for CFD*, Second ed., DCW Industries, Inc., (1994).
26. Bazargan M., and Mohseni M., "The Significance of the Buffer Zone of Boundary Layer on Convective Heat Transfer to a Vertical Turbulent Flow of a Supercritical Fluid", *The Journal of Supercritical Fluids*, **51**, PP 221-229(2009).
27. Song J.H., Kim H.Y., Kim H., and Bae Y.Y., "Heat Transfer Characteristics of a Supercritical Fluid Flow in a Vertical Pipe", *The Journal of Supercritical Fluids*, **44**, PP 164-171(2008).
28. Lemmon E.W., Peskin A.P., LcLinden M.O., and Friend D.G., "NIST 12: Thermodynamic and transport properties of pure fluids", *NIST Standard Reference Database Number 12*, (2003).

29. Bazargan M., and Mohseni M., "Effect of Turbulent Prandtl Number on Convective Heat Transfer to Turbulent Upflow of Supercritical Carbon Dioxide", *ASME Summer Heat Transfer Conference (HT2009)*, (2009).

30. McEligot D.M., Coon C.W., and Perkins H.C., "Relaminarization in tubes", *International Journal of Heat Mass Transfer*, **13**, PP 431-433(1970).

31. Lee J.I., Hejzlar P., Saha P., Kazimi M.S., and McEligot D.M., "Deteriorated Turbulent Heat Transfer (DTHT) of Gas Upflow in a Circular Tube: Experimental Data", *International Journal of Heat and Mass Transfer*, **51**, PP 3259-3266(2008).